

# Performance of a water-based liquid scintillator with a 1000-liter prototype detector

Aiwu Zhang<sup>a,\*</sup>, Lindsey J. Bignell<sup>a,\*\*</sup>, Milind V. Diwan<sup>a</sup>, David Jaffe<sup>a</sup>, Steve Kettell<sup>a</sup>, Richard Roesero<sup>b</sup>, Minfang Yeh<sup>b</sup>, Chao Zhang<sup>a</sup>

<sup>a</sup>Physics Department, Brookhaven National Laboratory, Upton, NY 11973, USA

<sup>b</sup>Chemistry Department, Brookhaven National Laboratory, Upton, NY 11973, USA

---

## Abstract

Water-based liquid scintillator (WbLS) is a new technology that combines both Cherenkov and scintillation processes in light production. It provides a cost-effective way to build large detectors that are sensitive to rare processes. At Brookhaven National Laboratory, we constructed and operated a 1000-liter detector exposed to cosmic rays and viewed by eight 2-inch PMTs. The detector was first filled with water and then transited to WbLS by adding organic liquid and mixing in-situ. The performances of both the water and the WbLS detectors are compared to a full Geant4-based simulation. A model describing the WbLS's light production, absorption and re-emission is provided and examined with the simulation. The WbLS stability is discussed.

**Keywords:** Water-based liquid scintillator (WbLS); Cherenkov process; scintillation process; light yield; attenuation length; Geant4 simulation.

---

## Contents

<b>1</b>	<b>Introduction</b>	<b>3</b>
<b>2</b>	<b>Detector prototype configuration</b>	<b>4</b>
2.1	Detector geometry arrangement . . . . .	4
2.2	Water circulation and purification system . . . . .	5
2.3	Data acquisition and monitoring system . . . . .	7
<b>3</b>	<b>WbLS production</b>	<b>9</b>
3.1	Production procedure . . . . .	9
3.2	WbLS light yield measurement with small samples . . . . .	9
3.3	Sixty-liter test stand . . . . .	9

---

\*Corresponding author: Tel. +1(631)344-5483; Email [azhang@bnl.gov](mailto:azhang@bnl.gov)

\*\*Now with ANU.

20	3.4	Mixing of WbLS in the 1000-liter detector . . . . .	9
21	<b>4</b>	<b>Detector commisioning</b>	<b>11</b>
22	<b>5</b>	<b>Data analysis</b>	<b>13</b>
23	5.1	Waveform analyses . . . . .	13
24	5.1.1	PMT gain stability during detector operation . . . . .	14
25	5.1.2	Pulse finding algorithm . . . . .	14
26	5.2	Event selection . . . . .	14
27	5.2.1	Event rate of different triggers . . . . .	14
28	5.2.2	Muon timing information . . . . .	14
29	5.2.3	Number of photons measured by the PMTs . . . . .	14
30	5.3	Environmental monitoring . . . . .	14
31	<b>6</b>	<b>Detector simulation</b>	<b>14</b>
32	6.1	The Rat-Pac framwork . . . . .	14
33	6.2	Muon generator . . . . .	15
34	6.3	The attenuation model for water . . . . .	15
35	6.4	The WbLS optical model . . . . .	15
36	<b>7</b>	<b>Results</b>	<b>15</b>
37	7.1	Water attenuation length . . . . .	15
38	7.2	WbLS attenuation and light yield . . . . .	15
39	<b>8</b>	<b>Summary and discussion</b>	<b>16</b>
40	<b>9</b>	<b>Conclusions</b>	<b>16</b>

## 1. Introduction

Over the past 25 years, the development and implementation of very large liquid-based particle detectors has led to some of the most important discoveries in fundamental physics in the neutrino sector. Table 1 summarizes several typical neutrino detectors that have been built in the world utilizing large volume of either water or liquid scintillator (LS) as detection medium. In all these detectors, either Cherenkov (for water) or scintillation (for LS) photons are detected .

Table 1: Typical neutrino experiments that use large volume (tonne-scale) water or liquid scintillators as detection medium. [I list the physics involved, maybe not accurate, can be removed.](#)

Experiment	Detector medium	scale	Physics involved	Reference
Super-Kamiokande <sup>1</sup>	Pure water	50 kton	$\theta_{23},  \Delta m_{32}^2 $	[1, 2]
SNO <sup>1</sup>	heavy water	1 kton	$\theta_{12},  \Delta m_{21}^2 $	[3]
KamLAND	Liquid scintillator	1 kton	$\theta_{12},  \Delta m_{21}^2 $	[4, 5]
Daya Bay	Liquid scintillator, Gd-loaded	20 ton $\times$ 8	$\theta_{13}, \Delta m_{32}^2$	[6, 7]
NO $\nu$ A	Liquid scintillator	8.8 kton	$\theta_{23}, \Delta m_{23}^2$	[8, 9]
PROSPECT	Liquid scintillator, <sup>6</sup> Li-loaded	5 ton	Reactor antineutrino spectrum, sterile neutrino	[10, 11, 12]

<sup>1</sup> These experiments made discovery measurement on neutrino oscillations and were awarded the 2015 Nobel prize in physics.

The concept of combining both Cherenkov and scintillation processes in a water-based liquid scintillator (WbLS) has been conceived in the middle of 1980s [13]. A WbLS is considerably interesting because it enhances rare event detection in the low energy interaction regions thanks to the scintillation process for energies that are below Cherenkov threshold. There have been recent developments aim at understanding the production and basic properties about WbLS [14, 15, 16, 17, 20]. The potential applications of WbLS have been discussed elsewhere [18] and could be established in experiments in THEIA [19], WATCHMAN [21] as examples.

As part of the investigation, a 1000-liter detector prototype, also called one-ton detector because its mass is near one ton, has been constructed at Brookhaven National Laboratory (BNL) for studying the feasibility of applying WbLS to future large experiments in many aspects. The one-ton detector is first filled with water and then with WbLS, it is exposed to cosmic rays and viewed by eight 2-inch PMTs (Hamamatsu R7723). In this paper, the construction and commissioning of the detector will be described in detail, the data between water and WbLS are compared with a Geant4-based simulation for understanding the WbLS's light yield and attenuation properties, the WbLS stability will also be discussed.

## 2. Detector prototype configuration

### 2.1. Detector geometry arrangement

The one-ton detector is built in the Physics Department at BNL, figure 1 shows the geometrical arrangement of the detector components, details about it are described below.

- A cylindrical acrylic vessel is used to contain the liquid. The vessel's inner diameter is 995 mm, its wall and bottom thicknesses are both 25.4 mm. The height of the vessel from the inner side of the bottom to the top is 1250 mm. The vessel has an earring ring with an outer diameter of 1150 mm for mounting a lid on top of the vessel. A 9.6 mm wide groove is opened in the earring ring at a diameter of 1068 mm that allows inserting a 3/8 inch (9.525 mm) O-ring as a seal when closing the lid.

- The lid itself is also made of 25.4 mm thick acrylic and has a diameter of 1150 mm matching the diameter of the earring ring of the vessel. Two holes of diameter 177.8 mm are opened in the lid, where two small cylindrical acrylic vessels (ports) of 25.4 mm wall thickness extend out by 100 mm. The distance between the centers of the two ports is 293.7 mm. The two vessels are used as a liquid buffer which ensure no air bubbles being trapped in the main vessel during filling liquid into the detector. They also allow liquid tubes go in and out for circulation and nitrogen cover gas tubes for flowing through the buffer regions.

- A 6.35 mm thick black teflon sheet (indicated in figure 2) is installed inside the main vessel covering the cylindrical surface to reduce the amount of photon reflection at the vessel wall.

- The detector is put on a frame made of 80/20 aluminum bars. At the bottom of the vessel, six 2-inch PMTs (Hamamatsu R7723) are mounted coupled by 2 mm thick optical cookies<sup>1</sup>. Two same type PMTs are mounted the same way viewing downwards at the top of the vessel. Four small plastic scintillator (PS) detectors are installed above the vessel for triggering cosmic rays, and two large PS detectors are installed under the vessel for selecting muons that go through the vessel. The six PS detectors consist a cosmic hodoscope system.

- The dimensions and relative locations of the PS and PMTs are described in figure 2. In the following of this paper, the PMTs and plastic scintillators are denoted as S0-S7 and H0-H5, respectively. S4 and S5 are the top PMTs while others are at the bottom, H0-H3 are the cosmic ray hodoscope detectors at the top whereas H4 and H5 are the large PS detectors at the bottom.

- Liquid float sensors are installed in the two port at fixed heights defining a liquid level range in the ports, these float sensors are replaced by ultrasonic level sensors (Senix ToughSonic30) which do not need to get in contact with the WbLS for better material compatibility.

- The entire detector is located in a dark room made of card boxes, and the floor is designed as a secondary container in case the 1000-liter liquid all gets out due to any type of leaks.

---

<sup>1</sup>Optical cookies EJ-560, <https://eljentechnology.com/products/accessories/ej-560>.

- A  $\sim 410$  nm LED is located on the top of the lid inbetween PMTs S4 and S5 for PMT calibration, and a temperature sensor (USB-TC01) is put at the top for monitoring temperature in the dark room.
- Nitrogen cover gas is introduced into the vessel for protecting WbLS. The tubes, as well as cables for high voltage, signal, LED and the temperature sensor, are routed out through a panel on the wall.

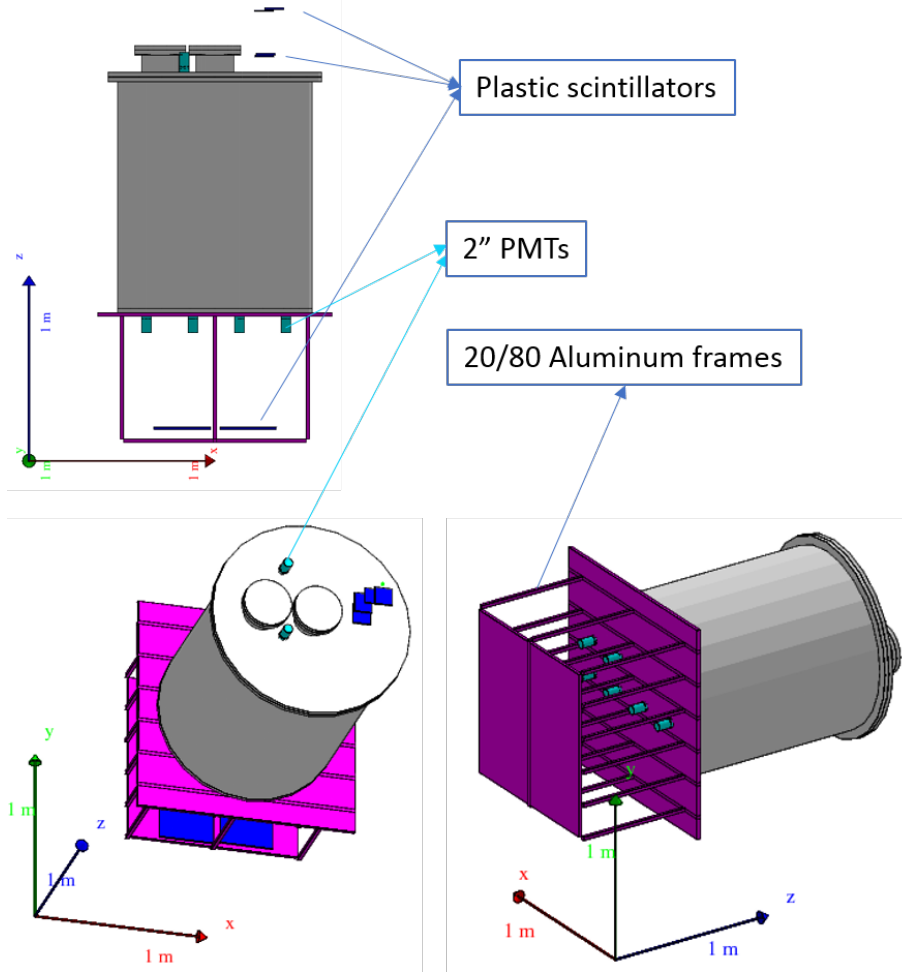


Figure 1: The 1000-liter prototype detector configuration viewing from different angles. The liquid vessel sits on an 80/20 aluminum frame. The detector has two PMTs viewing downwards from the top and six PMTs viewing upwards from the bottom. Four small plastic scintillators (PS) at the top form hodoscopic cosmic ray triggers and two large PS at the bottom help in selecting muons that pass through the detector. See details in the text and figure 2 about the dimensions.

## 2.2. Water circulation and purification system

As mentioned earlier, the detector is first filled with water. A water circulation and purification system is built as shown by the diagram in Figure 3. Tap water is pumped in and filtered by a pre-filter, a reverse osmosis (RO) filter and a deionisation filter. After the fill, water circulation continues to run and only the deionisation filter is involved. A degassing filter is inserted for removing air bubbles that dissolve in the

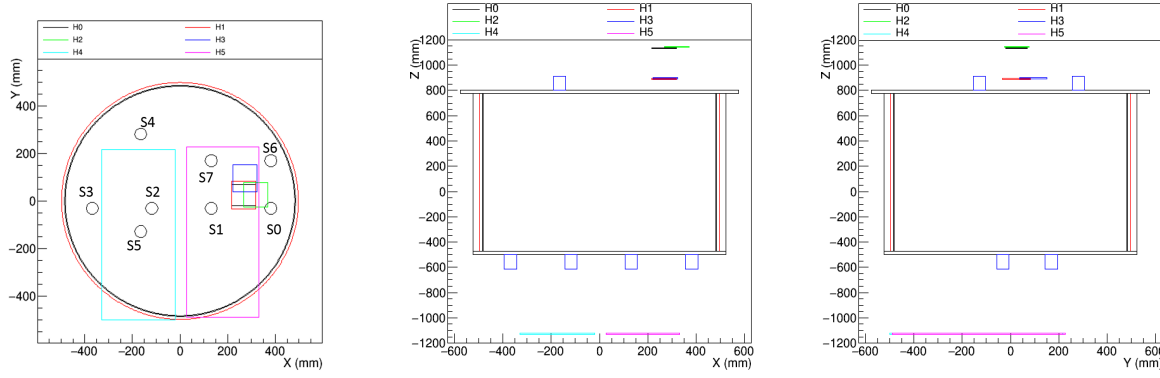


Figure 2: The dimensions and relative locations of plastic scintillator detectors and the PMTs. The plots from left to right show the views of the detector in X-Y, X-Z and Y-Z planes. In the X-Y plane, the large red circle is for the inner of the acrylic vessel, and the black circle next to it represent the black teflon sheet that surrounding the vessel to stop light reflection at the vessel wall. PMTs and plastic scintillator detectors are denoted as S0-S7 and H0-H5, respectively. The coordinate system shown here is used in the detector simulation.

water and a conductivity meter is included for monitoring the water quality. Water sampling points exist in the inlet and outlet tubes for taking water samples for light transparency measurements. The water is nearly pure and has been observed very stable for over long period of time. The monitored resistivity result is shown in figure 4, resistivity is seen improved after circulation tubing system being updated on 6/12/2018 (see discussion in section 4). [Water absorbance at one wavelength along time..](#)

The water level in the vessel will drop because of water evaporation and sampling, therefore, water will be manually added through the filling line once the level in the two small ports gets lower than a level float about 25.4 mm above the lid.

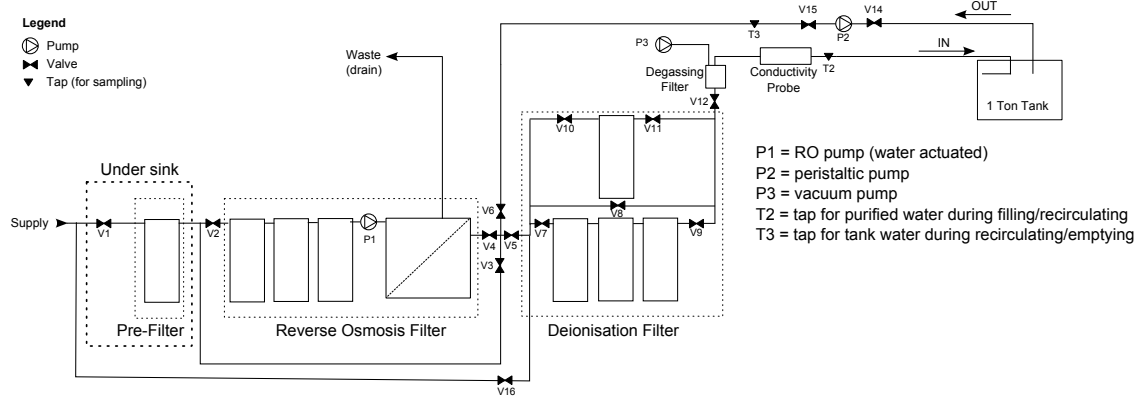


Figure 3: The water circulation and purification system for the 1000-liter water detector.

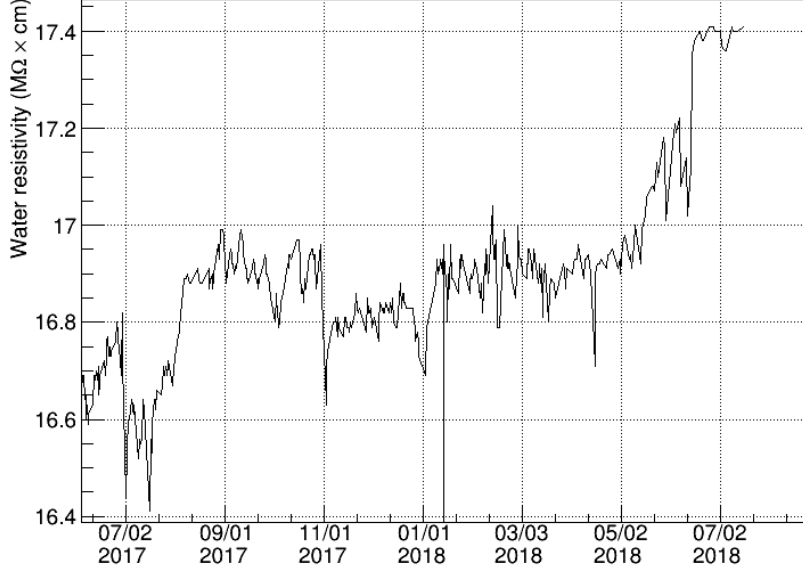


Figure 4: Water resistivity monitoring along time.

### 2.3. Data acquisition and monitoring system

The data acquisition (daq) focuses on recording PMT waveforms from cosmic events (mainly muons) and two trigger types are defined: hodoscope and multiplicity triggers. In addition, a third LED trigger is also set for PMT calibration. A hodoscope trigger is registered as  $(H2 + H0) \cdot (H3 + H1)$  meaning at least one in H2 and H0 is hit and at least one in H3 and H1 is hit, a multiplicity trigger is registered when  $\geq 6$  PMTs in the eight PMTs see pulses above a threshold of  $\sim 0.25$  photoelectron (p.e.). The threshold is set low because the expected number of photons is small in every PMTs. A LED trigger is fixed at 0.5 Hz to provide PMT calibrations at the single p.e. level, the LED is located at the top of the lid and is roughly in the middle of PMTs S4 and S5, from where the light comes out and reach all PMTs. When any of these three triggers becomes true, all PMT waveforms will be recorded by two CAEN digitizers (V1729A) and the time information of the triggered detectors is stored in a CAEN TDC module (V775) except for S6 and S7. The detailed trigger logic scheme is shown in figure 5, together with the digitizer and TDC information, charge (through CAEN V965A) and event rate (through CAEN V830) are also recorded.

The entire daq software is written in LabVIEW. Some simple monitoring parameters are implemented in the daq as well. These include the water conductivity as mentioned earlier, the temperatures inside the dark room and the electronics rack. When the detector is filled with water, two level floats are installed at fixed locations (one in the liquid and one above the liquid). When the detector is filled with WbLS (see section 3), the level floats are replaced by two ultrasonic level sensors (Senix ToughSonic30) mounted above the two small ports. An alarm email will be sent once water level is beyond the defined range. This ensures

129 that the detector is operated in a safe mode.

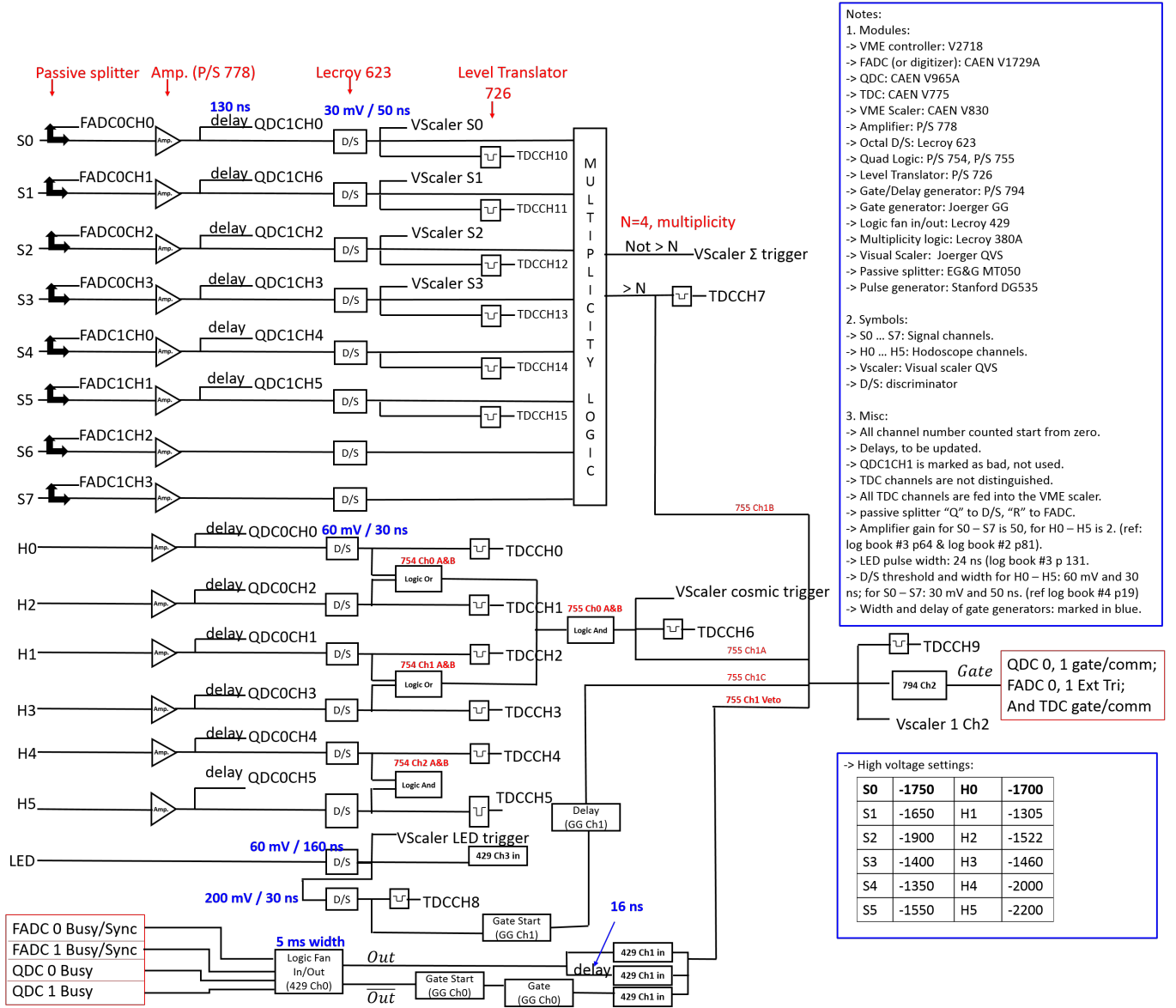


Figure 5: The detector trigger logic and data acquisition scheme. See text for detail descriptions.



### 3. WbLS production

#### 3.1. Production procedure

WbLS with 1% of liquid scintillator concentration by mass is the target of our studies. The WbLS production is divided into three steps<sup>1</sup>. First, certain amount of a surfactant is mixed with the liquid scintillator (LAB). The surfactant helps the dissolution of liquid scintillator into water. Second, the mixture from the previous step is added into pure water and the mixing process is continued until it is thoroughly mixed. For a 1-liter sample the mixing time of a couple hours is sufficient. In this step, the liquid will be cloudy and the third step will clear it by injecting a type of anti-scattering material and mixing for another shorter period of time.

The WbLS's absorbance is measured and its attenuation length is measured. [Measurement procedures will be described, plots will be shown, docdb242 has the basic information.](#)

#### 3.2. WbLS light yield measurement with small samples

[Using cosmic ray and a small test stand \(one 1/2 inch PMT\) and 10 mL samples, the light yield as a function of WbLS concentration is measured. I think this is useful information, for example, it provides basis on why 1% concentration is selected. I will expand it in this sub-section, docdb245 has the information.](#)

#### 3.3. Sixty-liter test stand

Instead of producing 1000-liter WbLS and replacing the water, it is favored that the WbLS to be produced by mixing in-situ with the existing 1000-liter purified water.

A 60-liter test stand is established in order to test the feasibility of the in-situ mixing idea. Figure 6 shows the relative absorbance of the WbLS samples at 400 nm wavelength during the mixing in this test stand. The circulation speed in this test is about 1 liter/s and it can be seen from the figure that the absorbance approaches a stable value which matches the value obtained from the previously WbLS made in 1-liter bottles. Therefore, this test gives use confidence that the in-situ mixing of the 1000-liter liquid would work.

#### 3.4. Mixing of WbLS in the 1000-liter detector

In the 1000-liter water circulation system (figure 3) PE tubing is used and is not suitable for in contact with liquid scintillator, also the degasser and the water conductivity meter are not compatible with WbLS, therefore the circulation system needs some modifications for WbLS in-situ mixing and circulation. New PTFE tubes and valves are added into the system as shown in figure 7, also ultrasonic level sensors are used for replacing the level floats as mentioned in section 2.3.

---

<sup>1</sup>The WbLS recipe is subjected to patent protection so no further details will be explained.

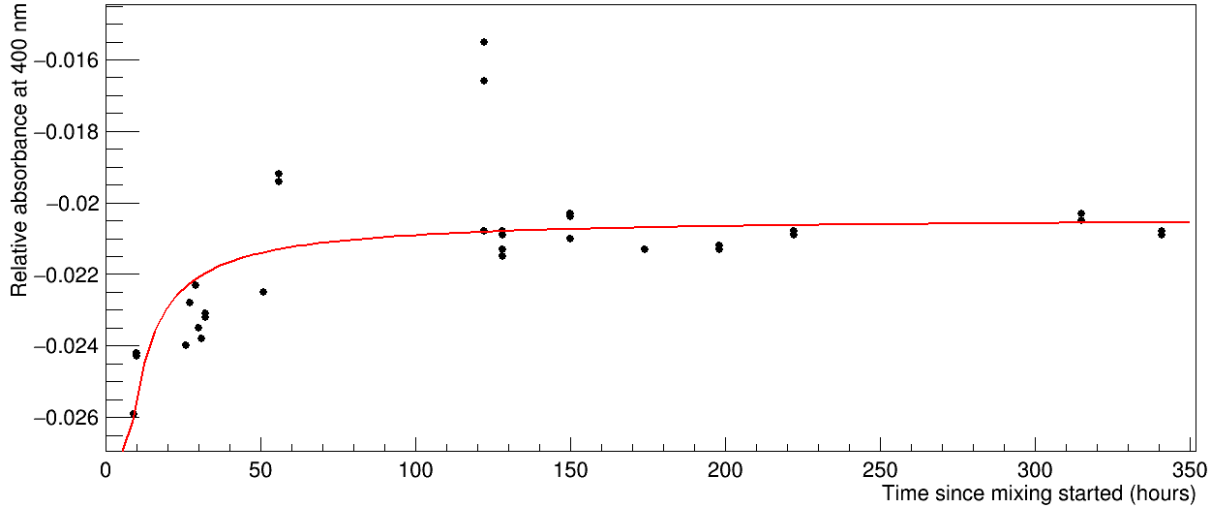


Figure 6: Relative absorbance of the 1%-WbLS samples along time during the mixing in the 60-liter test stand. The reason for negative absorbance values is explained in [12]. The red line is used as a guide line and the data points that much far away from this line is considered fluctuations in the measurement procedure.

Organic materials are added into the 1000-liter externally as depicted by the pink dashed-line box in figure 7. To produce  $\sim 1000$  liters of 1% WbLS to a good precision, a little more than 10 liters of organic materials are needed. Since the buffer region does not have the enough volume to contain all the organic materials in one fill, a few steps are planned and carefully conducted during operation, which ensured the success of achieving the goals of making 1% WbLS at a good precision and not introudcing air bubbles into the main vessel. When adding the first component (mixed liquid scintillator and surfactant), liquid level is monitored and the mass of the material containers (glass bottles) are measured after the operations to confirm that the correct mass is added into the vessel. When adding the second component (the anti-scattering agent), the amount that enters into the vessle is monitored by a precise scale and is also confirmed by the expected level change. The final concentration of the WbLS is conservatively estimated to be  $(1.00 \pm 0.02)\%$  after the operations.

It is worth to note the mixing of water and the first organic component takes three weeks (at a circulation speed of about 1.1 lter/min) until no chunks of organic material is seen. During the mixing process, samples are taken regularly for absorbance measurements to do a brief quality monitoring. Figure 8 shows a few absorbance curves in comparison with result from a 1% WbLS sample produced separately, absorbance values at 400 nm wavelength are also plotted along the mixing time in days.

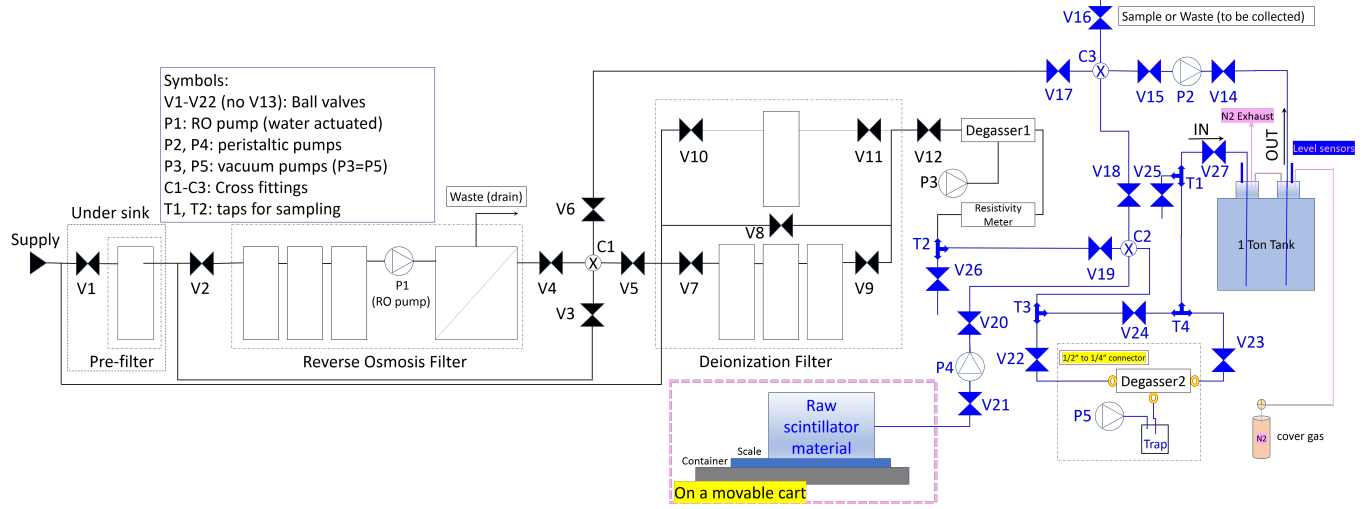


Figure 7: The modified circulation system that is suitable for WbLS. Comparing to figure 3, the tubes and valves in blue color are made of PTFE which is known compatible with liquid scintillator. A new degasser (Degasser2) is included and is not used in the end. The parts in the pink dashed-line box are used for adding organic materials into the main vessel for in-situ mixing of WbLS, and is removed after it is done.

#### 4. Detector commissioning

In this section, the operation and commissioning of the one-ton detector are described. [Some facts here first, I will write detailed operations in a better logic, but comments are welcomed to improve:](#)

The detector has been started with water since 2016, the eight PMTs were all installed on 8/22/2017, PMTs were calibrated and PMT gains are set to near  $1.2 \times 10^6$  and threshold is tuned to be around 0.25 p.e., optical cookies were updated on 11/8/2017, After tuning signal delays in daq, starting from 1/2/2018 the water data taking has started without any further changes in the detector settings.

On 6/12/2018, the circulation system dedicated for WbLS was updated and ultrasonic level sensors were installed. Water data were continued to be taken until 7/16/2018, when adding of organic liquid into the vessel began.

Time line for WbLS commissioning (figure 9):

- 7/16/2018, added first organic component (mix of liquid scintillator and surfactant);
- 7/31/2018, added anti-scatter agent;
- 8/6/2018, it was decided that the mixing was complete, and the inlet and outlet tubes that were down near the vessel bottom were pulled up. Data taking for the WbLS-filled detector began on that date, circulation was on;
- 8/27/2018, it is motivated that a real experiment with liquid detector should not have disturbances from circulation, so the circulation was turned off;

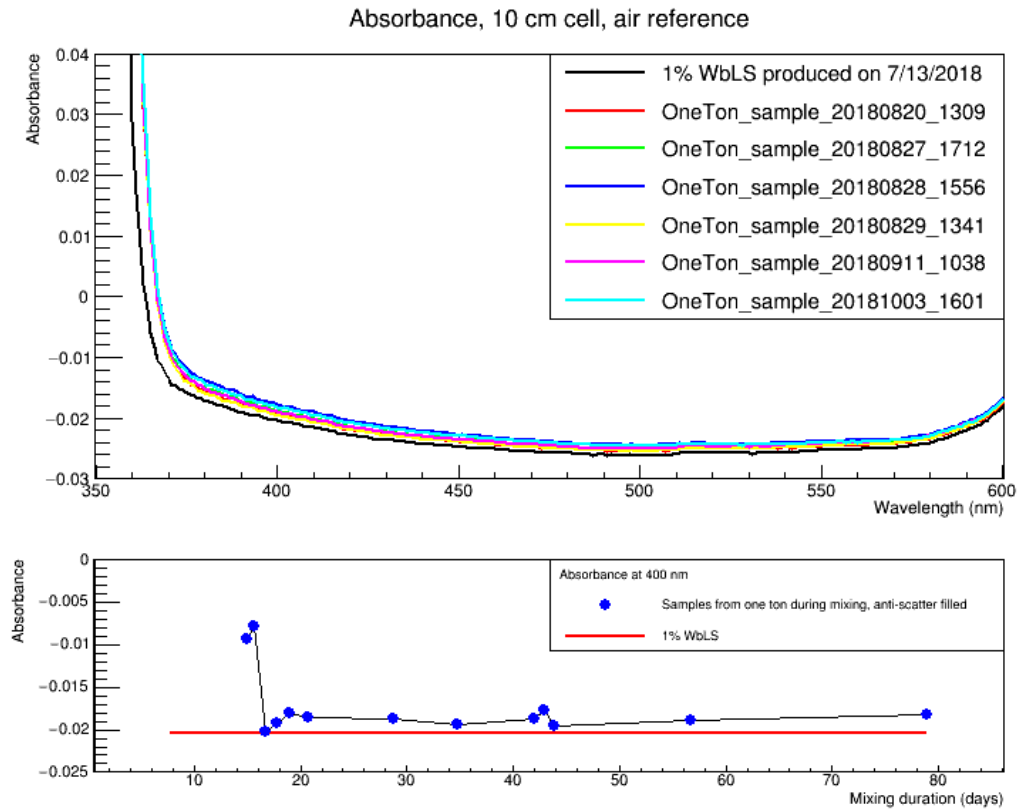


Figure 8: Absorbance curves of a few WbLS samples during the mixing, in comparison with a 1% WbLS sample produced separately (top), as well as Absorbance values at 400 nm wavelength for different samples along the time (bottom).

- 10/10/2018, the detector has been running fine thus far, and the liquid level has dropped down below the setting value (25.4 mm) because of sampling WbLS for absorbance monitoring, ~1.2 L pure water was added on this date. It is estimated that adding this amount of water will not change the WbLS concentration drastically (relative change is only about 0.12%).

- 11/2/2018, WbLS absorbance started getting worse after water was added, and it was considered further mixing was needed, so circulation was turned back on (the tubes were not pushed down however).

- 1/12/2019, stopped the circulation. During this circulating period, the pump was reported to have problems.

- 1/28/2019, the outlet tube was pushed down to near the vessel bottom (by 2 inch) and some samples were taken for absorbance measurements.

- 1/30/2019, the inlet tube was also pushed down for better circulation (but note the pump was not powerful enough).

- 4/8/2019, data taking was stopped.

- starting from the end of 08/2018, the multiplicity trigger data was only recorded at 1 to 2 days per week.

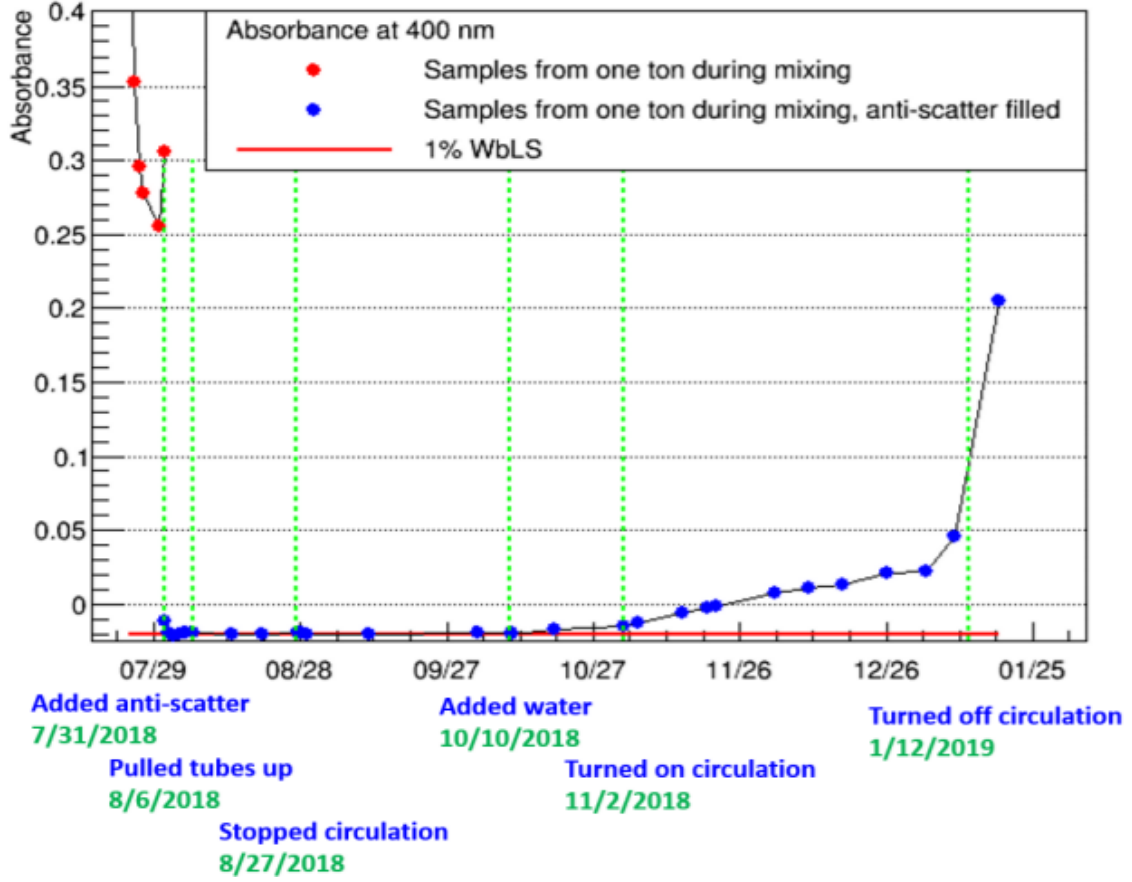


Figure 9: Absorbance values at 400 nm wavelength for all the samples taken during the operation of the 1000-liter WbLS detector. The green dashed lines are marking the time when some actions are taken, as described under the plot.

- 5/3/2019, WbLS was pumped out for detector decommissioning.

The water data taken between 1/2/2018 and 7/16/2018, and the WbLS data from 8/6/2018 to 10/10/2018, will be used for analysis; WbLS data after adding the water (10/10/2018) could be used for systematic uncertainty studies.

## 5. Data analysis

In the analyses, mainly the PMT waveforms and the TDC timing information are used, with the former for measuring number of photons and the later for triggering selection and timing.

### 5.1. Waveform analyses

An algorithm is developed to find the following information for the recorded PMT waveforms: number of pulses, start time, pulse amplitude and integral charge of every pulse. Using the LED triggers as calibration, the integral charge is measured as number of photoelectrons (npe).

#### 5.1.1. PMT gain stability during detector operation

The eight PMTs are stable over a period of more than one year has been achieved. The gain variation is less than 1%. A plot will be needed to show it.

#### 5.1.2. Pulse finding algorithm

#### 5.2. Event selection

##### 5.2.1. Event rate of different triggers

Plots to show event rate as function of time for hodoscope triggers, multiplicity triggers, LED triggers.

##### 5.2.2. Muon timing information

Timing information recorded by TDC and from PMT pulses.

##### 5.2.3. Number of photons measured by the PMTs

Plots to show npe distributions in PMTs, for different trigger types, for water and WbLS separately.

#### 5.3. Environmental monitoring

Plots showing temperature variation along time. Plots showing level change along time.

## 6. Detector simulation

### 6.1. The Rat-Pac framework

The processes of light production, attenuation, yield, absorption and reemission etc. in water as well as in WbLS are modeled in a Geant4 simulation and compared with the data in order to extract the values and uncertainties.

The Rat-Pac framework <sup>1</sup> is adopted in our study for its convenience of applying either water or liquid scintillator detectors and the simulation of photon measurements with PMTs.

In the simulation, properties of all other components, such as attenuation of acrylic, optical cookies, quantum efficiency of PMTs, and so on, are provided with either measurement of values from literatures.

The fixed inputs to the simulation:

- PMT quantum efficiency curve;
- Attenuation length and r-index of acrylic;
- r-index of water, and WbLS, is fixed;
- Besides, the black teflon's reflection probability is set to be 5% and very small attenuation length. So the effect from reflected photons from the wall is restricted to be very small.

---

<sup>1</sup>Rat-Pac reference: <https://rat.readthedocs.io/en/latest/>.

## 6.2. Muon generator

Muon samples are generated for the simulation. The generator used is the CRY package developed at LLNL [22].

The plots to show: muon momentum distribution, angle distributions.

## 6.3. The attenuation model for water

Describe the model with one parameter for attenuation length.

## 6.4. The WbLS optical model

The WbLS optical model:

Attenuation as a function of wavelength, it is measured by UV-vis. Will vary the spectrum to see how it fits with data

photon reemission probability (quantum yield), reemission wavelength spectrum (measured). Need a parameter for the quantum yield.

WbLS light yield itself is a parameter.

# 7. Results

## 7.1. Water attenuation length

Water attenuation length is fit by scanning the parameter in simulation and comparing to the npe distributions measured from the data.

The Gaussian form  $\chi^2$  with considering statistical uncertainties of simulation is used [23]:

$$\chi^2 = \sum_{i,j} \left( \frac{(m_i - \mu_i)^2}{m_i + \mu_i} \right)_j, \quad (1)$$

where  $m_i, \mu_i$  are for number of events in the  $i$ -th bin of the npe distributions, and  $j$  is for different exclusive trigger types selected by the plastic scintillator detectors. The number of bins used is 50, in order to avoid to small number of entries in the higher bins, the bins with <10 events (including the overflow bin) are combined as one bin in the  $\chi^2$  calculation.

A plot showing  $\chi^2$  as a function of the water attenuation parameter is needed. From which the water attenuation length is claimed to be measured.

npe distributions comparing data and MC for the best fit need to be shown.

## 7.2. WbLS attenuation and light yield

To be implemented.

## 8. Summary and discussion

## 9. Conclusions

## Acknowledgments

This work is supported by Brookhaven National Laboratory under \*\*\*. Many thanks to Xiangpan Ji, Hanyu Wei etc. for their insightful discussions and suggestions.

## References

- [1] The Super-Kamiokande Collaboration, Evidence for oscillation of atmospheric neutrinos, Phys. Rev. Lett. 81 (1998) 1562-1567.
- [2] The Super-Kamiokande Collaboration, The Super-Kamiokande detector, Nuclear Instruments and Methods in Physics Research Section A, 501 (2003), 418-462.
- [3] Q. R. Ahmad et al., Direct evidence for neutrino flavor transformation from neutral-current interactions in the Sudbury Neutrino Observatory, Phys. Rev. Lett. 89 (2002) Article 011301.
- [4] K. Eguchi et al., First Results from KamLAND: Evidence for Reactor Antineutrino Disappearance, Phys. Rev. Lett. 90 (2003) 021802.
- [5] S. Abe et al., Precision measurement of neutrino oscillation parameters with KamLAND, Phys. Rev. Lett. 100 (2008) 221803.
- [6] F. P. An et al., Observation of electron-antineutrino disappearance at Daya Bay, Phys. Rev. Lett. 108 (2012) 171803.
- [7] F. P. An et al., The detector system of the Daya Bay reactor antineutrino experiment, Nuclear Instruments and Methods in Physics Research Section A, 811 (2016), 133-161.
- [8] M. A. Acero et al., New constraints on oscillation parameters from  $\nu_e$  appearance and  $\nu_\mu$  disappearance in the NOvA experiment, Phys. Rev. D, 98 (2018) 032012.
- [9] S. Mufson et al., Liquid scintillator production for the NOvA experiment, Nuclear Instruments and Methods in Physics Research Section A, 799 (2015), 1-9.
- [10] J. Ashenfelter et al., First search for short-baseline neutrino oscillations at HFIR with PROSPECT, Phys. Rev. Lett. 121 (2018) 251802.
- [11] J. Ashenfelter et al., Measurement of the antineutrino spectrum from  $^{235}\text{U}$  Fission at HFIR with PROSPECT, arXiv: 1812.10877
- [12] J. Ashenfelter et al., Lithium-loaded liquid scintillator production for the PROSPECT experiment, JINST 14 (2019) P03026.
- [13] D. R. Winn and D. Raftery, Water-based scintillators for large-scale liquid calorimetry, IEEE Trans. Nucl. Sci., 32 (1) (1985), pp. 727-732.
- [14] M. Yeh et al., A new water-based liquid scintillator and potential applications, Nucl. Instrum. Methods A, 660 (1) (2011), pp. 51-56.
- [15] L. J. Bignell et al., Characterization and modeling of a water-based liquid scintillator, J. Instrum., 10 (12) (2015) P12009.
- [16] L. J. Bignell et al., Measurement of radiation damage of water-based liquid scintillator and liquid scintillator, J. Instrum., 10 (10) (2015) P10027.
- [17] Sun Heang So et al., Development of a liquid scintillator using water for a next generation neutrino experiment, Advances in High Energy Physics, Vol 2014, 327184.



- 313 [18] J. R. Alonso et al., Advanced scintillator detector concept (ASDC): A concept paper on the physics potential of water-based  
314 liquid scintillator, arXiv: 1409.5864.
- 315 [19] Vincent Fischer on behalf of the Theia collaboration, Theia: A multi-purpose water-based liquid scintillator detector,  
316 arxiv 1809.05987.
- 317 [20] J. Caravaca et al., Cherenkov and scintillation light separation in organic liquid scintillators, Eur. Phys. J. C (2017) 77:811.
- 318 [21] M. Askins et al., The physics and nuclear nonproliferation goals of WATCHMAN: A WAter CHerenkov Monitor for  
319 ANtineutrinos, arxiv 1502.01132.
- 320 [22] C. Hagmann, D. Lange, J. Verbeke and D. Wright, Cosmic-ray shower library (CRY),  
321 [https://nuclear.llnl.gov/simulation/doc\\_cry\\_v1.7/cry.pdf](https://nuclear.llnl.gov/simulation/doc_cry_v1.7/cry.pdf).
- 322 [23] R. Barlow and C. Beeston, Fitting using finite Monte Carlo samples, Comp. Phys. Comm. 77 (1993) 219-228.